# Petrology of contact metamorphosed argillite from the Rove Formation, Gunflint Trail, Minnesota

Theodore C. Labotka, J. J. Papike, D. T. Vaniman[1]

*Department of Earth and Space Sciences*
*State University of New York at Stony Brook*
*Stony Brook, New York 11794*

and G. B. Morey

*Minnesota Geological Survey*
*St. Paul, Minnesota 55108*

## Abstract

The contact metamorphic effects of the Duluth Complex on the argillaceous Rove Formation, northeastern Minnesota, are confined within a few hundred meters of the contact. The argillite has recrystallized from the low-grade assemblage chlorite + muscovite + quartz to assemblages characterized by cordierite + biotite + microcline + muscovite + quartz. Cordierite coexists with biotite over a wide range in Mg/(Mg + Fe) from 0.90 to less than 0.50. Andalusite is restricted to iron-rich rocks, although it occurs in one unusual magnesium-rich assemblage. Locally, corundum + microcline and cordierite + hypersthene assemblages occur at the contact with the Duluth Complex. The pressure, $P_{solid}$, of metamorphism is estimated to have been 1500 bars. The temperature near the contact ranged from ~500° to 600°C, based on the partitioning of Na and K between coexisting muscovite and microcline. The equilibrium constant for the continuous reaction muscovite + phlogopite + quartz = cordierite + microcline + $H_2O$ is calibrated and used to determine $f_{H_2O}$ attending metamorphism. Results indicate that $P_{H_2O}$ ranges from $P_{solid}$ to $\frac{1}{2}P_{solid}$. Calculation of the composition of COH fluid for a graphite-bearing sample indicates that the remainder of the fluid is mostly $CO_2$. The Rove Formation does not show the extensive mineralogic effects of contact metamorphism that the iron-formation shows, and the differences reflect the large thermal and compositional stability field for coexisting cordierite + biotite in pelitic rocks and the relatively small stability fields of the iron-rich minerals in the iron-formation.

## Introduction

The ~1 Gy Duluth Complex in northeastern Minnesota intruded an ~2 Gy sequence of sedimentary rocks that includes banded iron-formation (Gunflint–Biwabik) and argillite and greywacke (Rove–Virginia Formations). The contact metamorphic effects of the Duluth Complex on the iron-formation have been extensively studied by French (1968), Bonnichsen (1968, 1969), and Morey *et al.* (1972) (Biwabik Iron Formation), and by Simmons *et al.* (1974) and Floran and Papike (1975, 1978) (Gunflint Iron Formation). These iron-rich rocks are sensitive

to changes in metamorphic grade, and rocks as far away as 10 km (along strike) show effects of contact metamorphism. The zones of metamorphism recognized by French (1968) and Floran and Papike (1978) are low-grade zones characterized by greenalite or minnesotaite, intermediate-grade zones defined by grunerite- and fayalite-bearing assemblages, and a high-grade zone characterized by ferrohypersthene or inverted pigeonite.

The Rove Formation consists predominantly of carbonaceous argillite and quartz-rich greywacke, and the petrology of these rocks has been determined in order to compare the response of the more K- and Al-rich rocks to that of the iron-formation under low-pressure metamorphic conditions. In this report, the mineral assemblages and mineral compositions in

the Rove Formation are presented so that the distribution of elements among coexisting minerals in low-pressure, pelitic schists can be characterized. We use the mineral reactions that are inferred to have occurred to estimate the conditions of metamorphism.

## Geologic setting

The Rove Formation is part of a sequence of Proterozoic (~2Gy) sedimentary rocks assigned to the Animikie Group. The group unconformably overlies 2.7 Gy Archean rocks and consists of two units, the Gunflint Iron-Formation and the overlying Rove Formation. The stratigraphy and sedimentary petrography of the Rove Formation have been described by Morey (1969), and the general geology of northeastern Minnesota is shown in Figure 1.

The Rove Formation consists of a lower argillite unit, a middle transition unit, and an upper thin-bedded greywacke unit. The lower argillite unit is approximately 150 m thick and consists of thin-bedded, fissile, fine-grained greywacke, silty argillite, and graphitic argillite. Irregular limestone lenses and calcareous concretions also occur in the lower part of the unit. Beds of greywacke are abundant in the transition unit, and greywacke dominates the upper unit. The complete thickness of the two upper units is about 900 m, but the upper parts are generally truncated by the Duluth Complex in the region around Gunflint Lake.

The Duluth Complex, a composite mafic intrusion, truncates the rocks of the Animikie Group with slight angular discordance. Consequently, the complex is in
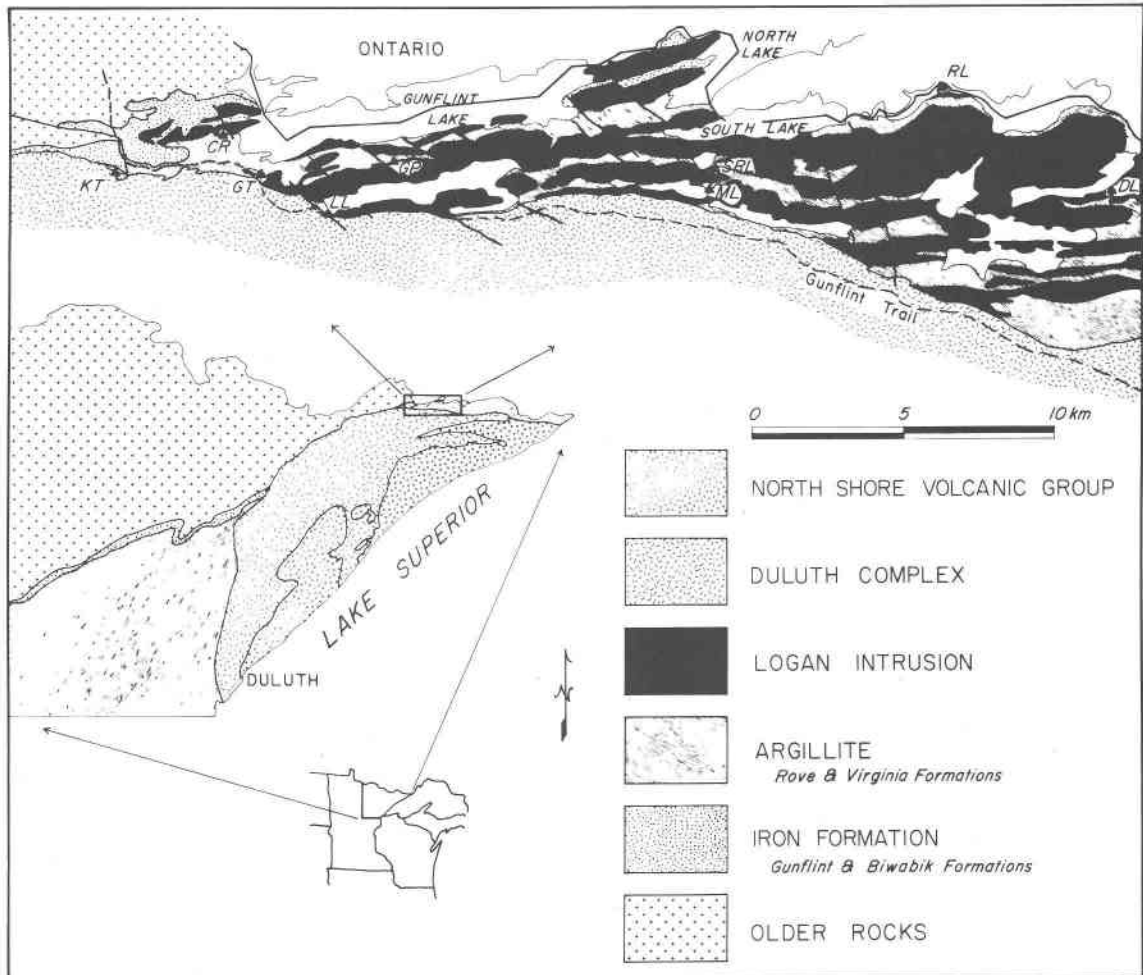


Fig. 1. General geology of the Gunflint Lake area, northeast Minnesota. Sample localities are indicated by the letters KT (Kakakebic Trail), CR (Cross River), GT (Gunflint Trail), LL (Loon Lake), GP (Gunflint Palisades), ML (Mayhew Lake), SRL (South Round Lake), RL (Rose Lake), and DL (Daniel's Lake).

contact with progressively higher units of the Animikie Group from west to east. Gabbroic sills and dikes assigned to the Logan Intrusions (Weiblen *et al.*, 1972) pervasively invade the Animikie Group in the vicinity of Gunflint Lake. The Logan Intrusions appear to be both older and younger than rocks of the Duluth Complex and are part of the same intrusive complex.

## Methods

The Rove Formation is not well exposed; outcrops generally only occur beneath the more resistant Logan sills or beneath the Duluth Complex adjacent to the contact. Samples were collected at sill contacts and in sequences away from the sills to determine the regional thermal environment and perturbations imposed by the sills.

The rocks were examined in thin section and the identification of some minerals was aided by X-ray diffractometry. Selected samples were analyzed with an ARL-EMX automated microprobe using simple silicate standards. Data were reduced on-line by the method of Bence and Albee (1968) and the correction factors of Albee and Ray (1970). Precision was monitored by analyzing minerals of known composition and is ~2% for major elements and ~10% for minor elements. Unknown minerals were analyzed in two or three areas on a standard thin section, and mineral compositions have ranges within the stated precision over the area of a thin section.

The structural state of potassium-feldspar has not been determined, and the use of the term "microcline" does not imply that K-feldspar has the triclinic structure.

## Mineral assemblages in pelitic rocks

Sample locations are shown on Figure 1, and the mineral assemblages in analyzed samples are given in Table 1. Rocks that exhibit only incipient recrystallization and retain detrital textures are termed "low grade." Rocks that have recrystallized to fine-grained hornfels are termed "medium grade," and those that show extensive interaction with the Duluth Complex are called "high grade."

The assemblages in quartz-bearing rocks can be represented in the system $K_2O$–$FeO$–$MgO$–$Al_2O_3$–$H_2O$. $H_2O$ is assumed to be a boundary-value component, and because either muscovite + quartz or microcline + quartz assemblages occur, mineral compositions may be projected onto the plane $FeO$–$MgO$–$Al_2O_3$ from either of these points to show the effects of Fe–Mg partitioning. These projections may be used as phase diagrams if the chemical potentials of $H_2O$ and each additional component are constant for all assemblages in each projection (Thompson, 1957).

### Low grade

The rocks from the Rove Formation are characterized by detrital textures except near the Duluth Complex and adjacent to some sills. The clastic grains in siltstones and greywackes have angular to subrounded shapes, and the matrix consists of fine- (<0.25 mm) to very fine-grained (<0.05 mm) micaceous minerals. The micaceous minerals chlorite, muscovite, and biotite have recrystallized from the presumably original clay matrix. The textures depend strongly on the rock type. The graphite-rich argillite near the base of the formation contains angular quartz and plagioclase grains, very fine-grained biotite and chlorite, and comparatively large (>0.5 mm) muscovite grains that have an idioblastic form and appear to be recrystallized detrital muscovite. In many samples, chlorite and muscovite are finely intergrown in the matrix. Albite grains are irregular in shape and contain fine-grained inclusions of epidote ("saussurite"). In some rocks, epidote occurs as distinct grains.

The observed mineral assemblages include quartz + muscovite + chlorite + biotite + plagioclase and quartz + muscovite + biotite + microcline + plagioclase. Rocks that were collected from Rose Lake and farther east, near Lake Superior, do not contain biotite. The diagnostic assemblage quartz + muscovite + chlorite + biotite + microcline + plagioclase occurs in sample 41s from South Round Lake. Graphite is very abundant in rocks from the lower part of the formation, near the western end of Gunflint Lake. All assemblages contain ilmenite or sphene and commonly pyrrhotite which is locally altered to marcasite. The chlorite-free assemblage quartz + muscovite + biotite + cordierite + plagioclase occurs in the Rove adjacent to the sill contact at South Round Lake.

Figure 2 illustrates the compositions of minerals that occur in muscovite + quartz-bearing assemblages from low-grade rocks of the Rove Formation. Chlorite + biotite coexist over a range in Mg/(Mg + Fe) from 0.65 to 0.50, biotite is slightly more iron-rich than coexisting chlorite, and microcline coexists with magnesium-rich chlorite. The low-grade sample 41e contains cordierite + biotite and indicates that near the sill chlorite has broken down at the composition Mg/(Mg + Fe) = 0.50.

Table 1. Analyzed samples, Rove Formation

| Sample | Quartz | Muscovite | Microcline | Biotite | Chlorite | Cordierite | Amphibole | Hypersthene | Al$_2$SiO$_5$[1] | Plagioclase | Others[2] |
|---|---|---|---|---|---|---|---|---|---|---|---|
| **LOW GRADE** | | | | | | | | | | | |
| Cross River | | | | | | | | | | | |
| 3 | X | X | | X | X | | | | | X | i,g |
| 43d | X | X | X | X | | | | | | X | i,g |
| 43f | X | | | X | X | | | | | X | ep,sph |
| South Round Lake | | | | | | | | | | | |
| 41e | X | X | | X | | X | | | | X | i,s |
| 41s | X | X | | X | X | | | | | X | r,s |
| Daniels Lake | | | | | | | | | | | |
| 42c | X | X | | | X | | | | | | |
| **MEDIUM GRADE** | | | | | | | | | | | |
| Gunflint Trail | | | | | | | | | | | |
| 22a | X | | X | X | | X | | | | X | i |
| 23 | | | | | | | | | | X | cpx,sph,s |
| 26 | X | | X | X | | X | | | | X | g,i,s |
| Mayhew Lake | | | | | | | | | | | |
| 35a | X | | | X | | | X | | | X | i,s |
| 35f | X | X | X | X | | X | | | | X | i,s |
| 35q | X | X | X | X | | X | | | | X | i,s |
| Loon Lake | | | | | | | | | | | |
| 39a | X | X | X | X | | X | | | | X | i,s |
| 39b | X | X | X | X | | X | | | | X | i,s |
| 39c | X | X | X | X | | X | | | | X | i,s |
| 39d | X | X | X | X | | X | | | | X | i,s |
| 39i | X | | | X | | | | X | | X | i,s |
| 39m | X | | | X | | | | X | | X | i,s |
| 39r | X | X | X | X | | X | | | | X | i,s |
| Gunflint Palisades | | | | | | | | | | | |
| 48f | X | X | X | X | | X | | | And | | g,s |
| **HIGH GRADE** | | | | | | | | | | | |
| Kakakebic Trail | | | | | | | | | | | |
| 16a | X | | | X | | X | | | | X | g,r |
| 16b | | | X | X | | X | | X | | X | i,g |
| 16i | X | | | X | | X | | | | X | r,g,s |
| 16j | X | | X | X | | | | X | | X | i,g |
| 18a | X | | X | X | | X | | | | X | i |
| 18b | X | | | X | | | | X | | X | i,s,cpx |
| 18c | | | X | | | X | | | Sil | | cor,gah,r,s |
| 18e | X | | | X | | | | | | X | g,s |

[1] And = Andalusite, Sil = Sillimanite
[2] i = ilmenite, r = rutile, sph = sphene, g = graphite, s = sulphide, cpx = diopside, cor = cordundum, gah = gahnite, ep = epidote

### Medium grade

At the localities of Mayhew Lake, Loon Lake, and Gunflint Trail adjacent to the Duluth Complex, rocks from the Rove Formation are completely recrystallized to fine-grained hornfels. All aspects of a sedimentary protolith, except compositional layering, have been obliterated. The most common mineral assemblage is quartz + muscovite + microcline + biotite + cordierite + plagioclase. The grain sizes of most minerals range from <0.10 mm to 0.25 mm, but muscovite occurs as porphyroblasts up to 1 mm in size.

At both Loon Lake and Mayhew Lake, closely spaced sequences of samples taken progressively farther from the contact show that the grain sizes of muscovite and biotite decrease from 1 mm to less than 0.25 mm within a distance of 20 m from the contact.

Cordierite occurs as ellipsoidal poikiloblasts, ~0.5 mm in diameter, that contain numerous quartz and feldspar inclusions. In many samples cordierite is altered to a yellowish chlorite. Plagioclase, microcline, and quartz are fine-grained (~0.1 mm), equigranular,
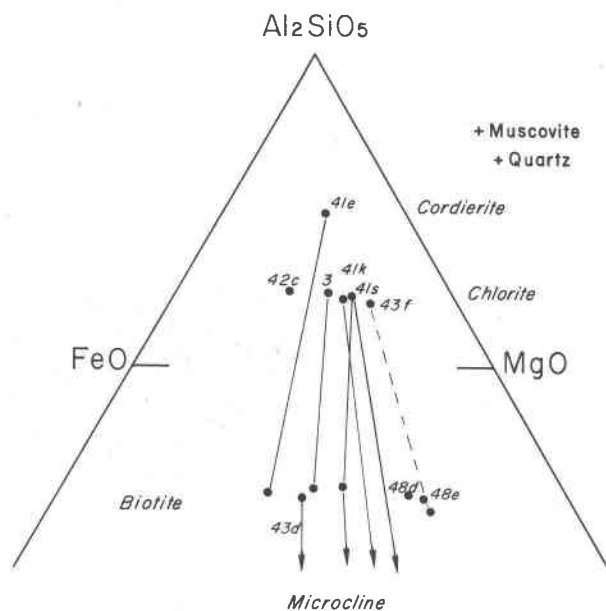
Fig. 2. Compositions of coexisting minerals in low-grade muscovite + quartz-bearing rocks.

and cannot easily be distinguished in thin section from one another. Pyrrhotite and ilmenite are additional minerals in all rocks, and graphite is locally present.

Because microcline occurs in most assemblages, the compositions of coexisting minerals are represented in Figure 3 in a projection from $KAlSi_3O_8$ and $SiO_2$. Muscovite compositions contain minor amounts of Mg and $Fe^{2+}$ (Table 2), but the range is too small to show on Figure 3; thus, muscovite is plotted at the apex of the triangle. The assemblage muscovite + cordierite + biotite occurs in the two suites of samples collected adjacent to sills at Mayhew Lake (35) and Loon Lake (39). Samples collected adjacent to the sills are labeled a, and samples collected progressively farther from the sills are labeled b, c, and so on. Samples from the Loon Lake locality are coarser-grained and closer to the high-grade region at Kakakebic Trail than the samples from the Mayhew Lake locality.

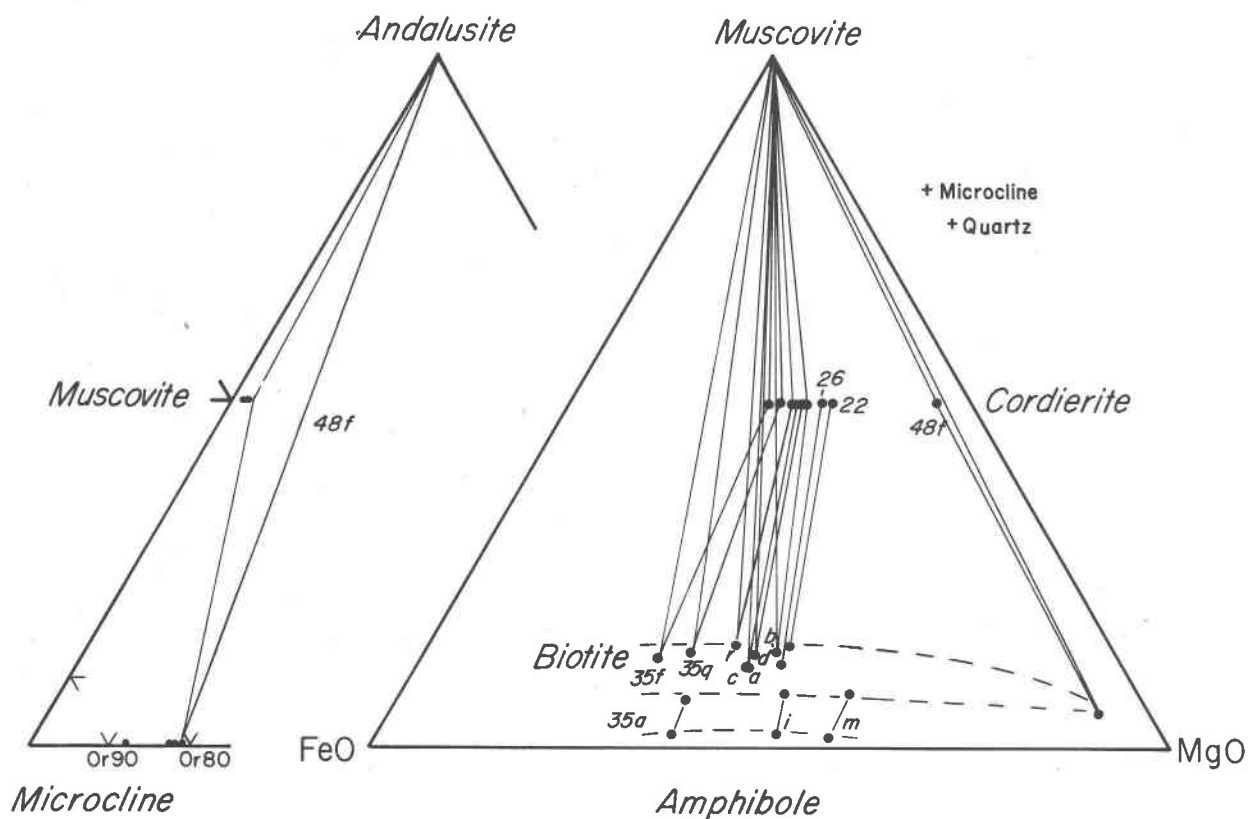The compositions of biotite and cordierite in the



Fig. 3. Compositions of coexisting minerals in medium-grade microcline + quartz-bearing rocks. Distribution of Na and K in muscovite + microcline + andalusite assemblage 48f also shown. Points labeled by letter only are samples 39. Biotite + cummingtonite assemblages do not contain microcline.

Table 2. Representative mineral compositions

| Sample | MUSCOVITE | | | | | | BIOTITE | | | | | | | CHLORITE | CORDIERITE | | | | | |
|---|---|---|---|---|---|---|---|---|---|---|---|---|---|---|---|---|---|---|---|---|
| | 3 | 35f | 35q | 39a | 39r | 48f | 3 | 16b | 35f | 35q | 39a | 39r | 48f | 3 | 16b | 35f | 35q | 39a | 39r | 48f |
| $SiO_2$ | 46.4 | 47.8 | 46.0 | 47.7 | 47.2 | 47.1 | 35.8 | 37.2 | 35.5 | 34.7 | 38.1 | 36.1 | 41.2 | 26.3 | 49.6 | 48.8 | 47.9 | 49.3 | 48.8 | 50.2 |
| $TiO_2$ | 0.1 | 0.1 | 0.0 | 0.5 | 0.3 | 0.5 | 1.5 | 5.0 | 3.8 | 4.0 | 3.8 | 2.3 | 0.8 | 0.4 | 0.0 | 0.0 | 0.1 | 0.0 | 0.0 | 0.0 |
| $Al_2O_3$ | 35.4 | 36.7 | 34.8 | 35.6 | 37.6 | 34.9 | 19.3 | 15.2 | 18.6 | 19.0 | 17.9 | 19.9 | 15.9 | 22.5 | 34.2 | 32.7 | 34.6 | 32.9 | 34.1 | 35.1 |
| MgO | 0.2 | 0.6 | 2.4 | 0.7 | 1.0 | 0.8 | 9.7 | 13.2 | 6.7 | 7.4 | 9.4 | 9.5 | 23.1 | 16.3 | 9.6 | 6.6 | 6.6 | 7.3 | 7.2 | 12.3 |
| FeO[1] | 2.2 | 0.9 | 3.0 | 0.8 | 0.7 | 0.1 | 17.1 | 16.4 | 22.5 | 21.1 | 19.1 | 19.2 | 2.8 | 22.3 | 6.8 | 11.3 | 10.9 | 10.0 | 10.2 | 2.2 |
| MnO | 0.0 | 0.0 | 0.0 | 0.0 | 0.0 | 0.0 | 0.1 | 0.1 | 0.0 | 0.0 | 0.0 | 0.0 | 0.0 | 0.2 | 0.0 | 0.0 | 0.1 | 0.1 | 0.1 | 0.1 |
| CaO | 0.0 | 0.0 | 0.0 | 0.0 | 0.0 | 0.0 | 0.0 | 0.0 | 0.0 | 0.0 | 0.0 | 0.0 | 0.0 | 0.0 | 0.1 | 0.0 | 0.0 | 0.0 | 0.0 | 0.0 |
| $Na_2O$ | 0.3 | 0.3 | 0.2 | 0.6 | 0.2 | 0.3 | 0.0 | 0.1 | 0.0 | 0.0 | 0.0 | 0.0 | 0.0 | 0.1 | 0.1 | 0.2 | 0.0 | 0.1 | 0.1 | 0.0 |
| $K_2O$ | 9.8 | 10.1 | 9.4 | 10.3 | 8.4 | 10.7 | 9.2 | 9.3 | 9.9 | 9.5 | 9.1 | 9.4 | 9.9 | 0.0 | 0.0 | 0.0 | 0.0 | 0.0 | 0.0 | 0.0 |
| $H_2O$[2] | 5.6 | 3.5 | 4.2 | 3.8 | 4.6 | 5.6 | 7.3 | 3.5 | 3.0 | 4.3 | 2.6 | 3.6 | 6.3 | 11.9 | | | | | | |
| Total | 100.0 | 100.0 | 100.0 | 100.0 | 100.0 | 100.0 | 100.0 | 100.0 | 100.0 | 100.0 | 100.0 | 100.0 | 100.0 | 100.0 | 100.4 | 99.6 | 100.2 | 99.7 | 100.5 | 99.9 |

FORMULA PROPORTIONS[3]

| | 3 | 35f | 35q | 39a | 39r | 48f | 3 | 16b | 35f | 35q | 39a | 39r | 48f | 3 | 16b | 35f | 35q | 39a | 39r | 48f |
|---|---|---|---|---|---|---|---|---|---|---|---|---|---|---|---|---|---|---|---|---|
| Si | 3.11 | 3.10 | 3.05 | 3.13 | 3.07 | 3.14 | 2.75 | 2.76 | 2.69 | 2.65 | 2.79 | 2.69 | 2.92 | 2.71 | 4.97 | 5.00 | 4.90 | 5.04 | 4.95 | 4.94 |
| Al | 2.79 | 2.81 | 2.72 | 2.75 | 2.89 | 2.74 | 1.75 | 1.33 | 1.66 | 1.71 | 1.55 | 1.75 | 1.33 | 2.73 | 4.03 | 3.96 | 4.17 | 3.97 | 4.08 | 4.06 |
| Ti | 0.01 | 0.01 | 0.00 | 0.02 | 0.01 | 0.03 | 0.09 | 0.28 | 0.22 | 0.23 | 0.21 | 0.13 | 0.04 | 0.03 | 0.00 | 0.00 | 0.00 | 0.00 | 0.00 | 0.00 |
| Mg | 0.02 | 0.06 | 0.24 | 0.07 | 0.09 | 0.08 | 1.12 | 1.46 | 0.75 | 0.84 | 1.02 | 1.05 | 2.44 | 2.50 | 1.43 | 1.01 | 1.01 | 1.11 | 1.09 | 1.80 |
| Fe | 0.12 | 0.05 | 0.17 | 0.04 | 0.04 | 0.01 | 1.10 | 1.01 | 1.43 | 1.35 | 1.17 | 1.20 | 0.17 | 1.91 | 0.57 | 0.97 | 0.93 | 0.85 | 0.87 | 0.18 |
| Mn | 0.00 | 0.00 | 0.00 | 0.00 | 0.00 | 0.00 | 0.01 | 0.00 | 0.00 | 0.00 | 0.00 | 0.00 | 0.00 | 0.01 | 0.00 | 0.00 | 0.00 | 0.00 | 0.01 | 0.01 |
| Ca | 0.00 | 0.00 | 0.00 | 0.00 | 0.00 | 0.00 | 0.00 | 0.00 | 0.00 | 0.00 | 0.00 | 0.00 | 0.00 | 0.00 | 0.01 | 0.00 | 0.00 | 0.00 | 0.00 | 0.00 |
| Na | 0.04 | 0.04 | 0.02 | 0.07 | 0.03 | 0.04 | 0.00 | 0.01 | 0.00 | 0.00 | 0.00 | 0.00 | 0.00 | 0.01 | 0.01 | 0.04 | 0.00 | 0.01 | 0.02 | 0.00 |
| K | 0.83 | 0.84 | 0.80 | 0.86 | 0.70 | 0.91 | 0.90 | 0.87 | 0.96 | 0.93 | 0.85 | 0.89 | 0.90 | 0.00 | 0.00 | 0.00 | 0.00 | 0.00 | 0.00 | 0.00 |

assemblage quartz + microcline + muscovite + cordierite + biotite range from relatively Mg-rich compositions for Loon Lake samples, in which biotite has an Mg/(Mg + Fe) ratio of about 0.50 and cordierite a ratio of about 0.65, to more Fe-rich compositions for Mayhew Lake samples in which biotite has an Mg/(Mg + Fe) ratio of 0.35 and cordierite a ratio of about 0.50. Because this assemblage quartz + microcline + muscovite + cordierite + biotite is invariant under constant $T$, $P$, and $\mu_{H_2O}$ conditions, the ob-

Table 2. (continued)

| Sample[1] | HYPERSTHENE | MICROCLINE | | | | | | PLAGIOCLASE | | | | | |
|---|---|---|---|---|---|---|---|---|---|---|---|---|---|
| | 16b | 16b | 35f | 35q | 39a | 39r | 48f | 3 | 16b | 35f | 35q | 39a | 39r |
| $SiO_2$ | 51.2 | 65.3 | 66.8 | 64.8 | 66.8 | 65.9 | 65.5 | 68.7 | 60.9 | 66.7 | 62.0 | 67.6 | 69.9 |
| $TiO_2$ | 0.2 | 0.0 | 0.0 | 0.0 | 0.0 | 0.0 | 0.0 | 0.0 | 0.0 | 0.1 | 0.0 | 0.0 | 0.0 |
| $Al_2O_3$ | 3.4 | 19.3 | 18.8 | 19.8 | 18.7 | 19.7 | 18.7 | 19.1 | 25.8 | 21.5 | 25.5 | 22.6 | 21.0 |
| MgO | 18.0 | 0.0 | 0.0 | 0.0 | 0.0 | 0.0 | 0.5 | 0.0 | 0.0 | 0.0 | 0.0 | 0.0 | 0.0 |
| FeO[2] | 26.3 | 0.2 | 0.2 | 0.2 | 0.2 | 0.4 | 0.0 | 0.2 | 0.2 | 0.3 | 0.2 | 0.1 | 0.2 |
| MnO | 0.3 | 0.0 | 0.0 | 0.0 | 0.0 | 0.0 | 0.0 | 0.0 | 0.0 | 0.0 | 0.0 | 0.0 | 0.0 |
| CaO | 0.2 | 0.2 | 0.0 | 0.0 | 0.0 | 0.0 | 0.1 | 0.3 | 7.3 | 2.9 | 5.5 | 2.7 | 0.7 |
| $Na_2O$ | 0.0 | 1.7 | 2.1 | 1.9 | 1.8 | 1.3 | 1.8 | 11.5 | 7.4 | 10.8 | 8.8 | 10.9 | 10.7 |
| $K_2O$ | 0.0 | 14.0 | 14.2 | 14.1 | 13.8 | 14.8 | 13.2 | 0.1 | 0.2 | 0.3 | 0.2 | 0.2 | 0.2 |
| $H_2O$[3] | | | | | | | | | | | | | |
| Total | 99.6 | 100.7 | 102.1 | 100.8 | 101.3 | 102.1 | 99.8 | 99.9 | 101.8 | 102.6 | 102.2 | 104.1 | 102.7 |

FORMULA PROPORTIONS[3]

| | 16b | 16b | 35f | 35q | 39a | 39r | 48f | 3 | 16b | 35f | 35q | 39a | 39r |
|---|---|---|---|---|---|---|---|---|---|---|---|---|---|
| Si | 1.94 | 2.97 | 3.00 | 2.95 | 3.01 | 2.97 | 3.01 | 3.00 | 2.67 | 2.88 | 2.70 | 2.86 | 2.97 |
| Al | 0.15 | 1.04 | 0.99 | 1.06 | 0.99 | 1.04 | 1.01 | 0.99 | 1.33 | 1.09 | 1.31 | 1.13 | 1.05 |
| Ti | 0.00 | 0.00 | 0.00 | 0.00 | 0.00 | 0.00 | 0.00 | 0.00 | 0.00 | 0.00 | 0.00 | 0.00 | 0.00 |
| Mg | 1.02 | 0.00 | 0.00 | 0.00 | 0.00 | 0.00 | 0.03 | 0.00 | 0.00 | 0.00 | 0.00 | 0.00 | 0.00 |
| Fe | 0.83 | 0.01 | 0.01 | 0.01 | 0.01 | 0.01 | 0.00 | 0.01 | 0.01 | 0.01 | 0.01 | 0.00 | 0.00 |
| Mn | 0.01 | 0.00 | 0.00 | 0.00 | 0.00 | 0.00 | 0.00 | 0.00 | 0.00 | 0.00 | 0.00 | 0.00 | 0.00 |
| Ca | 0.01 | 0.01 | 0.00 | 0.00 | 0.00 | 0.00 | 0.00 | 0.01 | 0.34 | 0.14 | 0.26 | 0.12 | 0.03 |
| Na | 0.00 | 0.15 | 0.18 | 0.17 | 0.16 | 0.12 | 0.16 | 0.98 | 0.62 | 0.90 | 0.74 | 0.89 | 0.88 |
| K | 0.00 | 0.81 | 0.82 | 0.82 | 0.79 | 0.85 | 0.78 | 0.00 | 0.01 | 0.02 | 0.01 | 0.01 | 0.01 |

[1] all Fe as FeO
[2] $H_2O$ by difference
[3] based on total positive charges of 12 (hypersthene), 16 (microcline and plagioclase), 22 (muscovite and biotite), 24 (chlorite), and 36 (cordierite)

served range in mineral compositions indicates that the rocks containing this assemblage equilibrated over a range in metamorphic grade. The positions of the three-phase fields on the AFM diagram in Figure 3 indicate the relative grades of metamorphism under which the various muscovite + cordierite + biotite assemblages formed. Displacement of the field is caused by the continuous dehydration reaction

muscovite + biotite + quartz = cordierite
$$+ \text{ microcline} + H_2O$$
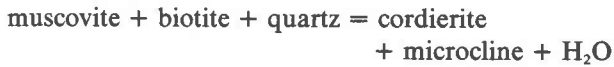
An increase in $T$ or a decrease in $\mu_{H_2O}$ drives this reaction to the right, and because biotite is more iron-rich than coexisting cordierite, the three-phase field cordierite + biotite + muscovite is displaced to more iron-rich compositions. Hence, the samples from Mayhew Lake (35f,q) formed under higher-grade conditions than the samples from Loon Lake (39a–r).

The relative difference in grade between the Loon Lake and Mayhew Lake localities is reversed from the anticipated difference based on the grain sizes and the distance from the high-grade Kakakebic Trail locality. An independent estimate of the relative grade is based on the partitioning of Na and K between coexisting muscovite and microcline (Fig. 4). Microcline is more Na-rich than coexisting muscovite, but the partition coefficient $K_D$ is not constant. $K_D$ is a function of temperature and composition, but because the range in Na/K for the coexisting phases is limited to K-rich compositions, $K_D$ is essentially a function of temperature. Because $K_D$ approaches 1.0 as temperature increases, samples from Mayhew Lake equilibrated at lower temperatures than the samples from Loon Lake. On the basis of compositions of coexisting cordierite and biotite, the lower-temperature Mayhew Lake samples formed at higher grade than the higher-temperature Loon Lake samples; thus variations in fluid composition strongly influenced the equilibrium muscovite + phlogopite + quartz = cordierite + microcline + $H_2O$.

The only andalusite-bearing rock (sample 48f) was collected from the Gunflint Palisades locality (Fig. 1) and contains the assemblage quartz + andalusite + cordierite + biotite + muscovite + microcline + ilmenite + graphite. Andalusite occurs as relatively large (1–2 mm) crystals with chiastolite habit in a graphite-rich matrix. The assemblage is unusual be-
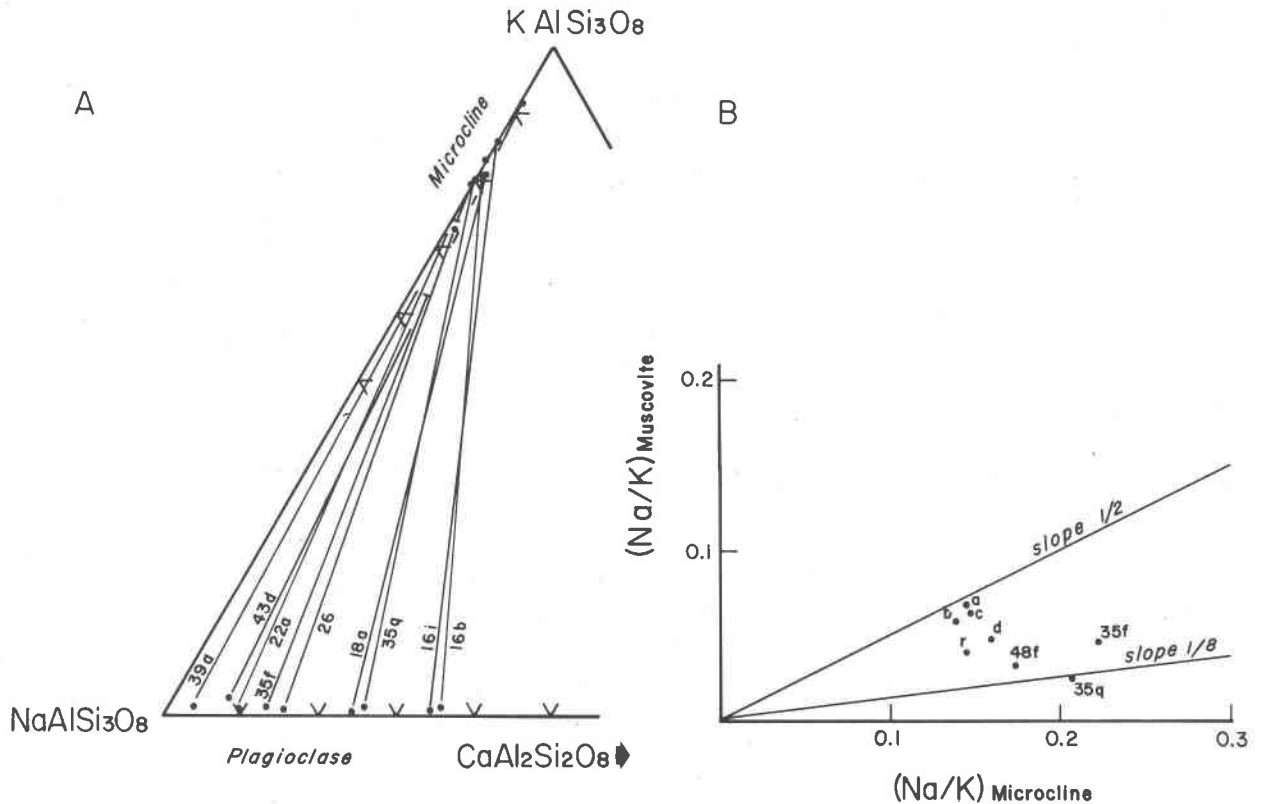


Fig. 4. (A) Compositions of coexisting feldspars, and (B) distribution of Na and K between coexisting microcline and muscovite.

cause the composition of biotite is very Mg-rich, and because the coexisting cordierite is more Fe-rich than biotite. The compositions of these minerals are given in Table 2 and shown on Figure 3. This reversal in Fe–Mg partitioning suggests that the assemblage may not have been in equilibrium, but there is no textural evidence for disequilibrium, and the compositional relationship between cordierite and biotite is constant over the area of a thin section. Mg-rich assemblages in pelitic schists are not well documented in the literature for comparison, and the assemblage in sample 48f is tentatively accepted as an equilibrium assemblage. Because plagioclase is absent, this assemblage indicates that in the calcium-free system the reaction muscovite + albite + quartz = andalusite + microcline + $H_2O$ has occurred. In the medium-grade rocks at Loon Lake muscovite coexists with plagioclase as sodic as $An_{12}$; therefore andalusite and microcline coexist only in very Na-rich, Ca-poor rocks.

The partitioning of Fe and Mg between coexisting cordierite and biotite in medium-grade and high-grade samples is illustrated in Figure 5a. In all samples except number 48f biotite is more Fe-rich than coexisting cordierite, but the magnitude of the distribution coefficient seems to depend on composition.

Guidotti *et al.* (1975a) find no dependence of $K_D$ on composition for coexisting cordierite + biotite + muscovite (no microcline) in very magnesium-rich pelitic schists, and Guidotti *et al.* (1975b) also find no relation between $^{VI}Al$ and Mg/(Mg + Fe) in biotite. Figure 5b shows an inverse correlation between Mg/(Mg + Fe) and $^{IV}Al$ which is a gauge of the amount of substitution of cations other than Fe and Mg in biotite. Herein lies the reason for the compositional dependence of $K_D$. If the Al content of biotite is constant, then the partition coefficient may be directly related to the equilibrium constant for the exchange reaction

$$\alpha\text{Mg-biotite} + \beta\text{Fe-cordierite} = \alpha\text{Fe-biotite} + \beta\text{Mg-cordierite}$$

where $\alpha$ and $\beta$ are the numbers of exchangeable cations in cordierite and biotite, respectively. The equilibrium constant is $(a_{\text{Fe-biotite}})^\alpha(a_{\text{Mg-cord}})^\beta/(a_{\text{Mg-biotite}})^\alpha(a_{\text{Fe-cord}})^\beta$. If the Fe–Mg solutions are ideal, then the equilibrium constant equals $(K_D)^{\alpha\beta}$ (Albee, 1972) and $K_D$ is independent of composition. If, however, some of the Fe in biotite is associated with octahedral Al, then this Fe cannot exchange with Mg in cordierite, and $K_D$ is not related in a simple way to the equilibrium constant for the exchange reaction. Instead of
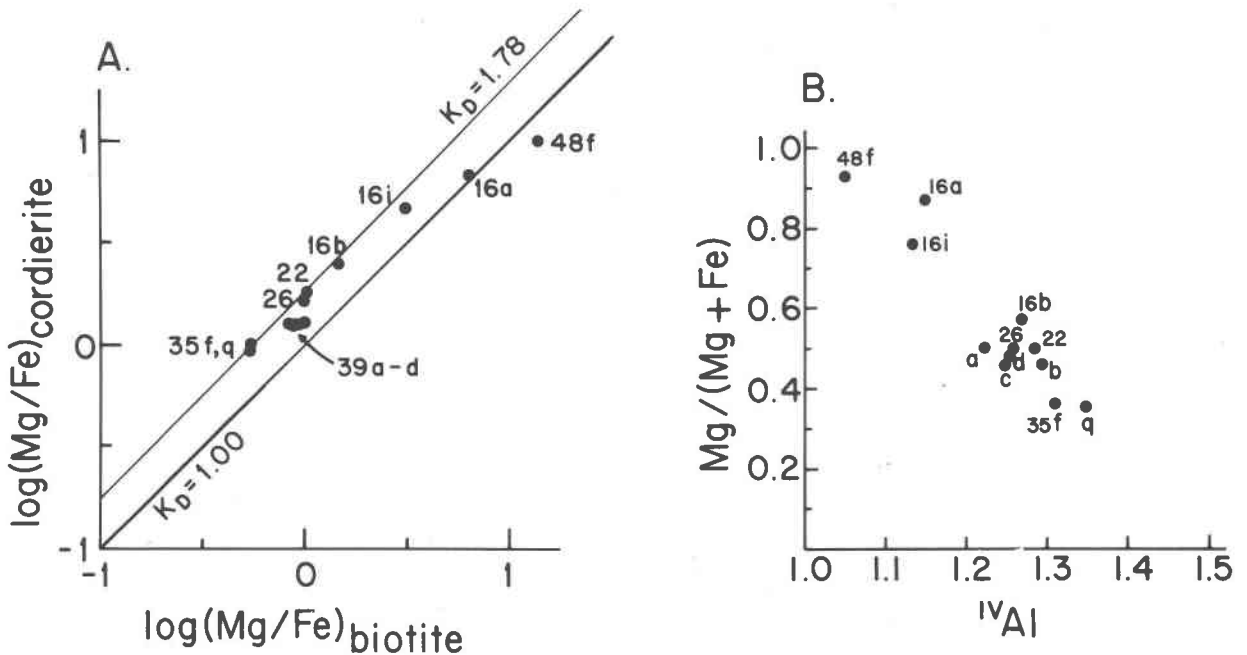


Fig. 5. (A) Distribution of Fe and Mg between coexisting cordierite and biotite in medium-grade and high-grade rocks. Cordierite is generally more Mg-rich than biotite except for the Mg-rich sample 48f. The lines $K_D = 1.00$ and $K_D = 1.78$ are shown for reference. (B) Inverse correlation between Mg/(Mg + Fe) and $^{IV}Al$ content in biotite.

two components related by the substitution of Fe for Mg, biotite from the Rove Formation contains additional components that relate an increase in Al and Ti to an increase in Fe. In this case, $X_{Fe}^{bio}$ includes Fe from both the annite and the other components, and $K_D$ will be different from the equilibrium constant for the exchange reaction in which only the mole fraction of annite is considered.

The assemblage quartz + biotite + cummingtonite + plagioclase occurs in two samples from Loon Lake (39) and one from Mayhew Lake (35). The amphibole is very fine-grained and is intergrown with the quartz + plagioclase matrix. Microcline does not coexist with cummingtonite, but the compositions of coexisting biotite and amphibole are shown on Figure 4 to illustrate the partitioning of Fe and Mg between them.

### High grade

Rocks from the Kakakebic Trail show the greatest degree of recrystallization, and some show extensive interaction with the Duluth Complex during emplacement. Here the Duluth Complex intruded the lower, carbonaceous part of the Rove Formation so that graphite has recrystallized to 0.25 to 0.50 mm grains. Cordierite forms spherical porphyroblasts with no inclusions and unusual twin patterns. Plagioclase grains are ~0.25 mm in diameter and have polygonal forms.

Several samples show a variety of textures within small areas and contain unusual assemblages that indicate assimilation and reaction of the Rove with the gabbro. There are regions in sample 16b that contain tabular, igneous plagioclase, and adjacent regions in which the plagioclase forms a polygonal aggregate. The shapes of hypersthene grains range from subhedral with few inclusions to very irregular poikiloblasts.

Pelitic rocks near the contact with the Duluth Complex contain the muscovite-free assemblage quartz + biotite + cordierite + K-feldspar + plagioclase + rutile + graphite + pyrrhotite. The compositions of coexisting cordierite + biotite in K-feldspar-bearing rocks are shown in Figure 6.

Most of the Rove Formation that crops out on Kakakebic Trail occurs as inclusions in the contact zone with the gabbro. The assemblage in these hybrid rocks is quartz + biotite + K-feldspar + hypersthene + plagioclase + ilmenite + graphite + pyrrhotite. The compositions of coexisting biotite and hypersthene are shown on Figure 6. Many pelitic rocks adjacent to the gabbro are deficient in quartz
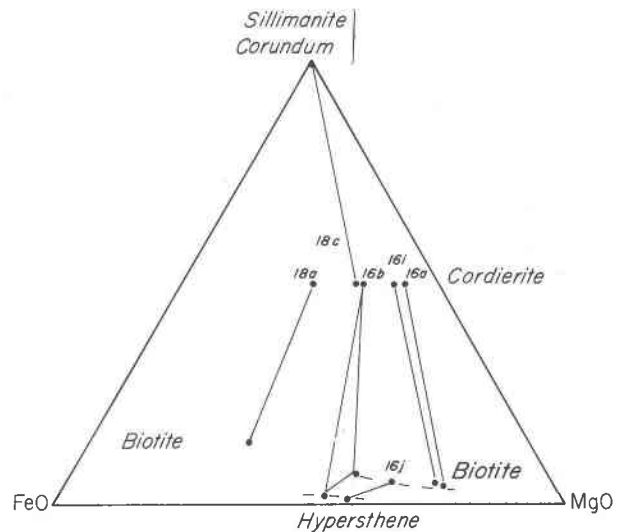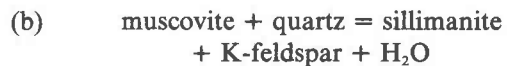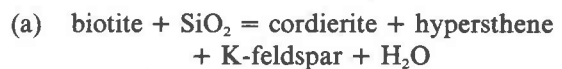


Fig. 6. Distribution of Fe, Mg, and Al among minerals in high-grade rocks. Samples 18c and 16b do not contain quartz. Samples 16a and 16i do not contain microcline.

and suggest that the silica-rich country rock has reacted with the silica-poor Duluth Complex. Assemblages in two of the analyzed rocks are cordierite + biotite + hypersthene + K-feldspar + plagioclase + ilmenite + graphite + pyrrhotite (16b) and cordierite + sillimanite + corundum + K-feldspar + Zn spinel (gahnite) (18c). The compositions of these quartz-free assemblages are also shown in Figure 6. Pelitic schists have interacted with the gabbro through the reactions

(a)   biotite + $SiO_2$ = cordierite + hypersthene
+ K-feldspar + $H_2O$

(b)        muscovite + quartz = sillimanite
+ K-feldspar + $H_2O$

and

(c) muscovite = corundum + K-feldspar + $H_2O$.

The activity of $SiO_2$ in sample 18c was buffered by the reaction

sillimanite = corundum + $SiO_2$.

In sample 16b the ratio $f_{H_2O}/a_{SiO_2}$ was determined by the compositions of coexisting biotite + cordierite + hypersthene + K-feldspar through reaction (a).

### AKFM facies series

In well-documented studies of contact- or low-pressure regional metamorphism of pelitic schists (Santa Rosa, Nevada, Compton, 1960; Steinach, Ba-

varia, Okrusch, 1969; Alsace, Bosma, 1964; Buchan, Read, 1952; Abukuma, Miyashiro, 1958) biotite + andalusite is a very common assemblage, and Labotka (1978) demonstrated for the Panamint Mountains that rocks with Mg/(Mg + Fe) in the range 0.35 to 0.56 contain andalusite. The rarity of andalusite-bearing assemblages in the Rove Formation was puzzling in light of these studies. However, in the Rove Formation muscovite + quartz + cordierite is stable over a large range in Mg/(Mg + Fe) from 0.09 to 0.50, and the biotite that coexists with the most iron-rich cordierite has Mg/(Mg + Fe) = 0.35. Microcline also coexists with this biotite + cordierite + muscovite assemblage, and because the four minerals are related by the continuous reaction

$$\text{muscovite} + \text{biotite} + \text{quartz} = \text{cordierite} + \text{microcline} + H_2O$$
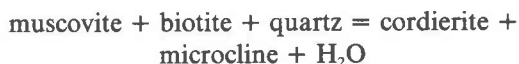
muscovite cannot coexist with magnesium-rich biotite. Thus, andalusite in pelitic schists is restricted to iron-rich compositions. These phase relations are similar to those reported by Tilley (1924) for the contact metamorphism of pelitic schists in the Comrie area, Scotland.

The facies series for progressive contact metamorphism of the Rove Formation is shown in Figure 7a–b. This series progresses from the low-grade assemblage muscovite + quartz + chlorite + biotite + microcline to the medium-grade assemblage muscovite + quartz + biotite + cordierite + microcline. The reaction sequence is based on the observed order of increasing Fe content in coexisting minerals: cordierite, chlorite, biotite. The unusual Mg-rich assemblage in sample 48f is neglected. The order of the generalized reactions assumes that $H_2O$ is evolved with increasing grade:

(1) chlorite + microcline = biotite + muscovite + quartz + $H_2O$
(2) chlorite + andalusite + quartz = cordierite + $H_2O$
(3) muscovite + chlorite + quartz = andalusite + biotite + $H_2O$
(4) chlorite + muscovite + quartz = cordierite + microcline + $H_2O$
(5) chlorite + microcline + quartz = cordierite + biotite + muscovite + $H_2O$
(6) chlorite + muscovite + quartz = cordierite + andalusite + biotite + $H_2O$
(7) biotite + muscovite + quartz = cordierite + microcline + $H_2O$

Figure 7c illustrates a slightly different sequence of reactions if reaction 1 goes to completion over the entire range in Mg/(Mg + Fe) before reaction 4 occurs.

Figure 7 predicts a variety of assemblages that ought to have formed in rocks with compositions on the plane chlorite + muscovite + quartz but are not observed; *viz.* chlorite + cordierite + microcline and chlorite + cordierite + biotite. Low-grade assemblages in pelitic rocks include chlorite, chlorite + biotite, or rarely chlorite + biotite + microcline, and these react to chlorite-free cordierite + biotite assemblages with no apparent intermediate steps. Either the intermediate reactions that limit the stability of chlorite occur over a very narrow temperature interval, or the intermediate reactions were overstepped because of the rapid temperature rise during emplacement of the gabbro complex. The total mass transfer recorded in these rocks is the sum of the intermediate reactions: chlorite + muscovite + quartz → biotite + cordierite + microcline + $H_2O$. The coefficients in this mass-balance relation depend on the bulk-rock composition.

## Intensive parameters

### Pressure and temperature

Pressure, temperature, and activities of volatile components may be calculated from the compositions of coexisting phases in the assemblage quartz + biotite + muscovite + cordierite + microcline + ilmenite + graphite + pyrrhotite which occurs at the Gunflint Palisades, Loon Lake, and Mayhew Lake localities. Pressure estimates can be made from the estimated thickness of overburden at the time of metamorphism. The Duluth Complex was emplaced near the surface, and the aggregate stratigraphic thickness of the gabbroic rocks and overlying volcanic rocks near Lake Superior was 15 km. However, Weiblen and Morey (personal communication, 1979) infer that both the plutonic and extrusive rocks thin northward to near zero thickness in the vicinity of Gunflint Lake. Simmons *et al.* (1974) estimated a minimum pressure of 2.0 kbar during metamorphism of the underlying Gunflint Iron Formation, a pressure that is based on the composition of iron-rich pigeonite produced during metamorphism.

A calcsilicate rock (sample 23) which occurs at the Gunflint Trail locality contains the assemblage diopside + anorthite + sphene + sphalerite + pyrite + chalcopyrite, and an additional estimate of the attending pressure may be based on the FeS content of sphalerite. Scott (1973, 1975) calibrated the composition of sphalerite that coexists with pyrite and pyr-
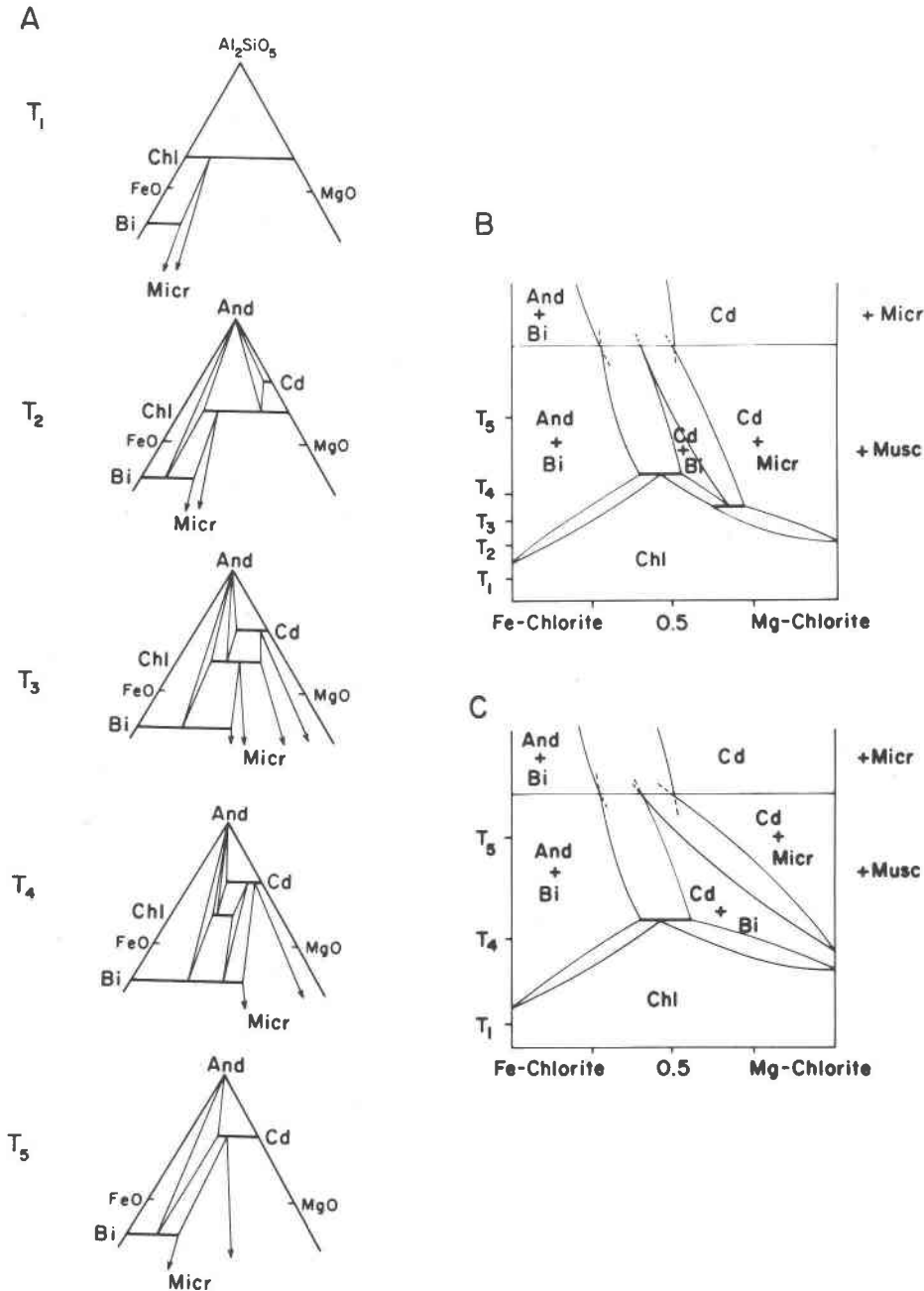
Fig. 7. Generalized facies series for the low-pressure, contact metamorphism of the Rove Formation. (A) Facies types for muscovite + quartz-bearing rocks. Low-grade rocks are represented by $T_1$, (although the three-phase field biotite + chlorite + microcline occurs at more Mg-rich compositions) and medium-grade rocks are represented by $T_5$. High-grade rocks are not represented. (B) Pseudobinary $T$-$X$ diagram on the join chlorite + muscovite + quartz for the facies series shown in A. (C) $T$-$X$ diagram for an alternate facies series in which the reaction chlorite + microcline = biotite + muscovite + quartz + $H_2O$ goes to completion over the entire range in Mg/(Mg + Fe) before chlorite begins to break down to cordierite + biotite.

rhotite for pressures (independent of temperature except at high temperatures) down to 2.5 kbar. Pyrrhotite does not occur in sample 23, so that the FeS content in sphalerite indicates a maximum pres-

sure. The composition is $Zn_{0.77}Fe_{0.23}S$ and indicates that the maximum pressure was less than 2.5 kbar. Metamorphism of the Rove Formation probably occurred at a pressure of 1.5 kbar. This value is the

minimum pressure suggested by Simmons *et al.* (1974) minus 0.5 kbar, because of the higher stratigraphic position of the Loon and Mayhew Lake samples relative to the Gunflint Iron Formation.

Temperatures may be calculated from the compositions of coexisting plagioclase and alkali feldspar, and the calibration of Powell and Powell (1977) has been used for several localities that contain assemblages with coexisting feldspars (Table 3). These feldspar temperatures are generally consistent with metamorphic grade, but their absolute values seem low in comparison with estimates from the stability

Table 3. Temperatures calculated from coexisting K–Na–Ca phases

| SAMPLE | PLAGIOCLASE | | | MICROCLINE | | | MUSCOVITE | | $K_D^1$ | $T^2$ | $T^3$ |
|---|---|---|---|---|---|---|---|---|---|---|---|
| | $X_{ab}$ | $X_{an}$ | $X_{or}$ | $X_{ab}$ | $X_{an}$ | $X_{or}$ | $X_{musc}$ | $X_{par}$ | | °C | °C |
| 16b | 0.640 | 0.350 | 0.010 | 0.156 | 0.008 | 0.836 | | | | 547 | |
| 16j | 0.650 | 0.340 | 0.010 | 0.180 | 0.010 | 0.810 | | | | 566 | |
| 18a | 0.752 | 0.239 | 0.009 | 0.142 | 0.001 | 0.857 | | | | 490 | |
| 22a | 0.897 | 0.096 | 0.007 | 0.193 | 0.000 | 0.807 | | | | 497 | |
| 26 | 0.837 | 0.151 | 0.012 | 0.261 | 0.011 | 0.728 | | | | 557 | |
| 35f | 0.857 | 0.129 | 0.014 | 0.182 | 0.001 | 0.817 | 0.954 | 0.046 | 4.61 | 513 | 548±10 |
| 35q | 0.733 | 0.253 | 0.014 | 0.169 | 0.001 | 0.830 | 0.976 | 0.024 | 8.27 | 555 | 484±10 |
| 39a | 0.870 | 0.119 | 0.011 | 0.168 | 0.001 | 0.831 | 0.924 | 0.076 | 2.45 | 482 | 620±5 |
| 39b | | | | 0.142 | 0.000 | 0.858 | 0.940 | 0.060 | 2.59 | | 613±7 |
| 39c | | | | 0.128 | 0.000 | 0.872 | 0.941 | 0.059 | 2.34 | | 627±7 |
| 39d | | | | 0.150 | 0.000 | 0.850 | 0.955 | 0.045 | 3.74 | | 568±10 |
| 39r | 0.954 | 0.033 | 0.013 | 0.120 | 0.000 | 0.880 | 0.961 | 0.039 | 3.58 | 418 | 570±10 |
| 43d | 0.900 | 0.072 | 0.028 | 0.081 | 0.002 | 0.917 | | | | 379 | |
| 48f | | | | 0.116 | 0.000 | 0.884 | 0.971 | 0.029 | 4.39 | | 544±12 |

$$^1 \quad K_D = \frac{(X_{musc}^{mica} X_{ab}^{micr})}{(X_{par}^{mica} X_{or}^{micr})}$$

$^2$ Temperature calculated from coexisting feldspars (Powell and Powell, 1977).

$$T = \frac{-(X_{or}^{micr})^2 \, [\, 6330 + 0.093p + 2X_{ab}^{micr} \, (1340 + 0.019p) \,]}{R\ln\left(\dfrac{X_{ab}^{micr}}{X_{ab}^{plag}}\right) + (X_{or}^{micr})^2 \, (-4.63 + 1.54 \, X_{ab}^{micr})}$$

$^3$ Temperature calculated from coexisting muscovite and microcline (Thompson, 1974).

$\Delta\mu^X/RT = 6.4894 - (6119.54/T)$

$\Delta\mu^X = (\mu_{musc} - \mu_{par}) - (\mu_{or} - \mu_{ab}) = RT\ln K_D + (W_{Gms} - W_{Gor}) + 2(W_{Gpa} - 2W_{Gms})X_{musc}^{mica}$

$+ 3(W_{Gms} - W_{Gpa})(X_{musc}^{mica})^2 - 2(W_{Gab} - 2W_{Gor})X_{or}^{micr} - 3(W_{Gor} - W_{Gab})(X_{or}^{micr})^2$

$W_{Gab} = 6326.7 + 0.0925p - 4.6321T$ \qquad Waldbaum and Thompson (1969)
$W_{Gor} = 7671.8 + 0.1121p - 3.8565T$

$W_{Gpa} = 3082.1 + 0.0822p + 0.1698T$ \qquad Eugster et al. (1972)
$W_{Gms} = 4163.9 + 0.1259p + 0.3954T$

Errors represent a ±10% error in the wt.% $K_2O$ in muscovite

p = 1500 bars

of pigeonite in the iron-formation: 547°C from sample 16b at the gabbro contact based on coexisting feldspars, and 800°C from Simmons *et al.* (1974) based on pigeonite stability.

Thompson (1974) calculated the Na–K exchange potential, $\Delta\mu$, for the reaction muscovite + albite = paragonite + orthoclase, and temperatures may also be calculated from the compositions of coexisting muscovite and microcline. He calculated two expressions for $\Delta\mu$. The first is derived from end-member dehydration curves, but predicts unrealistically low temperatures ($\sim-25$°C) for the metamorphism of the Rove Formation. The second exchange potential is derived from ion-exchange experiments and predicts temperatures that are similar to but generally higher than temperatures calculated from coexisting feldspars (Table 3). The muscovite–microcline temperatures are consistent with the geologic setting of the samples. Sample 35f which is adjacent to the contact of a large sill gives a temperature of 548°C, and sample 35q which is 5 m from the contact gives a temperature of 484°C. Sample 39a which is very coarse-grained gives a temperature of 620°C; this temperature is greater than that from sample 35f which is finer-grained and farther from the high-grade area near Kakakebic Trail.

The errors of ±10°C in the muscovite-microcline temperature are calculated from a generous ±10% error in the wt.% $K_2O$ in muscovite. Realistic errors in the temperature estimates are difficult to evaluate because of the lack of agreement between the two-feldspar and muscovite–microcline values, and because the other calibration of the muscovite–microcline exchange potential by Thompson (1974) gives unrealistic results. The muscovite–microcline temperatures for samples 39a,b,c are very close to the dehydration of muscovite + quartz, which suggest that they are too high and that the associated errors must be greater than those derived from analytical uncertainty. The errors in temperatures calculated from the two-feldspar calibration of Stormer (1975) and Powell and Powell (1977) are probably also large because the thermometer is relatively insensitive to the albite content in plagioclase at temperatures less than 600°C (Fig. 3 in Stormer, 1975). The actual temperatures during metamorphism may have been much lower than the muscovite–microcline value, but they were probably higher than the two-feldspar value.

*Volatile-phase composition*

The medium-grade samples from Loon Lake (39) are coarse-grained, record higher muscovite–micro-cline temperatures, and are closer to the high-grade region than samples from Mayhew Lake (35), but the compositions of coexisting biotite and cordierite in these samples indicate that the Mayhew Lake samples recrystallized at a "higher grade." Thus, regional variation in the composition of the fluid phase must have affected the relation

muscovite + biotite + quartz = microcline + cordierite + $H_2O$.
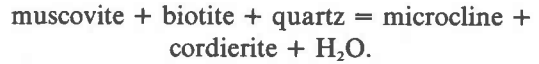
Portions of the system $MgO–Al_2O_3–K_2O–SiO_2–H_2O$ have been experimentally investigated by Schreyer, Yoder, Seifert, and others, and the data have been summarized by Schreyer and Seifert (1969). Schreyer and Seifert (1967) reported the results of experiments for the reaction muscovite + phlogopite + quartz = cordierite + microcline + $H_2O$ which seems to have occurred at 1 kbar, 550°±15°C, 2 kbar, 600°±15°C, 3 kbar, 670°±15°, 4 kbar, 690°±15°, and 5 kbar, 710°±10°C ($P_{H_2O} = P_T$). These data were fitted to a relation $0 = (A/T) + B + (CP/T) + \ln f_{H_2O}$, in which C is the volume change of solid phases divided by the gas constant. The least-squares result is

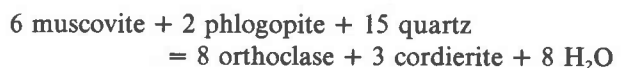$$0 = (1.126 \times 10^4/T) - 19.96 + (0.128P/T) + \ln f_{H_2O}$$

The total variance, $\sigma^2 = \Sigma(\text{predicted value} - \text{measured value})^2/(\text{degrees of freedom})$, is 358, which predicts temperatures within the error estimated for the location of the reaction. This relation can then be extended to include the effects of solid solution:

$$0 = (9.004 \times 10^4/T) - 159.7 + (1.022P/T) + \ln K_{eq}$$

where

$$\ln K_{eq} = 8 \ln a_{or}^{feld} + 3 \ln a_{Mg\text{-}cord}^{cord} + 8 \ln f_{H_2O} - 6 \ln a_{music}^{mica} - 2 \ln a_{phlog}^{bio}$$

for the stoichiometry

6 muscovite + 2 phlogopite + 15 quartz
= 8 orthoclase + 3 cordierite + 8 $H_2O$

The fugacity of $H_2O$ for a given temperature and pressure may be determined from the compositions of coexisting phases in the assemblage muscovite + microcline + cordierite + biotite + quartz, provided that the activity–composition relations for the minerals are known.

The activity–composition relations of Waldbaum and Thompson (1969) for alkali feldspars and of Eugster *et al.* (1972) for white micas have been used, and cordierite is considered to behave ideally ($a_{Mg\text{-}cord} = X_{Mg}^2$). The inverse correlation of Mg and $^{IV}$Al contents in biotite from the Rove Formation (Fig. 5b)

Table 4. $f_{H_2O}$ in medium-grade Rove Formation

| SAMPLE | T[1] | CORDIERITE | BIOTITE | | | | | | MUSCOVITE[2] | MICROCLINE[2] | $f^3$ $H_2O$ | $f^4$ $H_2O$ |
|---|---|---|---|---|---|---|---|---|---|---|---|---|
| | °C | $X_{Mg}$ | Ti | $^{VI}Al$ | $^{VI}\square$ | Mg | Fe | $X_{Mg}$ | RTln$\gamma$ <br> mica <br> musc | RTln$\gamma$ <br> feld <br> micr | bars | |
| 35f | 548 | 0.51 | 0.22 | 0.35 | 0.25 | 0.75 | 1.43 | 0.25 | 4.52 | 45.82 | 252 | |
| 35q | 484 | .0.52 | 0.23 | 0.36 | 0.22 | 0.84 | 1.35 | 0.28 | 1.20 | 47.42 | 83 | |
| 39a | 620 | 0.56 | 0.20 | 0.30 | 0.30 | 1.03 | 1.17 | 0.34 | 12.78 | 26.99 | 903 | |
| 39b | 613 | 0.58 | 0.09 | 0.44 | 0.14 | 1.19 | 1.14 | 0.40 | 7.82 | 17.43 | 1126 | |
| 39c | 627 | 0.56 | 0.20 | 0.36 | 0.26 | 1.02 | 1.16 | 0.34 | 7.55 | 12.36 | 954 | |
| 39d | 568 | 0.60 | 0.17 | 0.43 | 0.25 | 1.02 | 1.13 | 0.34 | 4.32 | 20.54 | 422 | |
| 39r | 570 | 0.56 | 0.13 | 0.44 | 0.18 | 1.05 | 1.20 | 0.35 | 3.22 | 16.89 | 423 | |
| 48f | 544 | 0.91 | 0.04 | 0.25 | 0.10 | 2.44 | 0.17 | 0.81 | 1.76 | 15.32 | 379 | 483 |

[1] Temperature derived from coexisting muscovite and microcline, Table 3.

[2] $RTln\gamma_1 = (1-X_1)^2(W_{G1}+2(W_{G2}-W_{G1})X_1)$. X and $W_G$ for muscovite and microcline are given in Table 3.

[3] $f_{H_2O}$ calculated from the equilibrium 6 muscovite + 2 phlogopite + 15 quartz = 3 cordierite + 8 microcline + 8 $H_2O$.

[4] $f_{H_2O}$ calculated from the equilibrium muscovite + quartz = andalusite + microcline + $H_2O$ (Chatterjee and Froese, 1975).
p = 1500 bars.

suggests that all Mg occurs as the phlogopite component. The activity of phlogopite in biotite is assumed to equal the cube of the mole fraction of Mg in the octahedral site.

The fugacities of $H_2O$ calculated from the above expression for eight medium-grade samples are given in Table 4. The temperatures used in the calculation are those derived from the muscovite–microcline equilibrium. These temperatures are maximum temperatures, and the fugacities calculated from them represent maximum possible values of $f_{H_2O}$ during metamorphism of these samples.

Samples 39a,b,c from Loon Lake give $f_{H_2O}$ values close to (or exceeding) the values for pure $H_2O$ at 1500 bars (Burnham et al., 1969). The samples from Mayhew Lake (35) and Gunflint Palisades (48f) give values much lower than the pure-$H_2O$ value.

Figure 8 illustrates the ranges of possible values of P, T, and $f_{H_2O}$ for samples 35f, 39a, and 48f. These values are determined by the biotite–cordierite–muscovite–microcline equilibrium, and the temperatures derived from the muscovite–microcline exchange equilibrium are superimposed to show the error in $f_{H_2O}$ resulting from a ±15° error. The equilibrium between muscovite–microcline–andalusite (Chatterjee

and Froese, 1975) for sample 48f is also presented to show the relative correspondence between the two equilibria. Figure 8 shows that the calculated values of $f_{H_2O}$ depend very strongly on temperature, but not on pressure. For example, an error in T of ±15°C for sample 35f results in an error of ±50 bars in $f_{H_2O}$ but an error in $P_{solid}$ of 500 bars results in an error of only ±22 bars in $f_{H_2O}$. Figure 8 also shows that in sample 48f for $P_{H_2O} = P_{solid}$ the biotite–cordierite equilibrium occurs at higher temperatures than the muscovite–aluminosilicate equilibrium. This topology violates Schreinemakers' rules and indicates that the *relative* error between the two equilibria is at least 25°C. Thus, even if the temperature is well known, the value of $f_{H_2O}$ at $P_{solid}$ = 1500 bars is only precise within a range of 100 bars. For example, values of $f_{H_2O}$ calculated for sample 48f at 544°C are 379 bars and 483 bars from the cordierite–biotite and muscovite–andalusite equilibria respectively (Table 4). The uncertainty is larger at greater rock pressures. The total uncertainty in the maximum $f_{H_2O}$ for sample 48f resulting from error in the maximum temperature and in calibration of the biotite–cordierite equilibrium is ±100 bars.

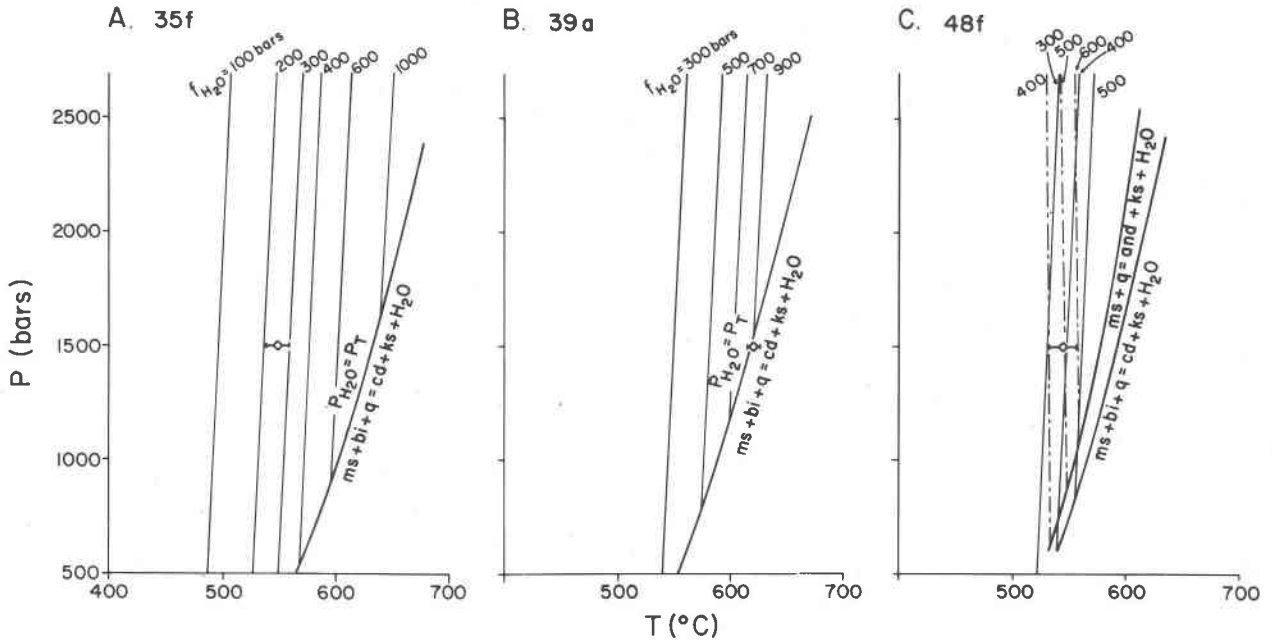Sample 48f contains graphite and if $P_{fluid} = P_{solid}$

Fig. 8. The equilibrium muscovite + biotite + quartz = cordierite + microcline + $H_2O$ for samples 35f (A), 39a (B), and 48f (C). Muscovite–microcline temperatures are given to show the effects of an error of ±10% on $K_2O$ in muscovite on the calculated $f_{H_2O}$. The equilibrium muscovite + quartz = andalusite + microcline + $H_2O$ for sample 48f is also shown in C to illustrate the relative error between the equilibria for determining $f_{H_2O}$. Broken lines in C correspond to the muscovite–andalusite equilibria.

and if C–O–H gas species are the only important components in the fluid phase, then the composition of the fluid phase can be calculated by the method reviewed by Eugster (1977). The results for the maximum values of $f_{H_2O}$ are given in Table 5. At $P_{fluid}$ = 1500 bars the maximum fraction of $H_2O$ in the fluid is 0.65±0.10, and most of the remainder of the fluid is $CO_2$. The composition of the fluid at 500°C is also given in Table 5 to show that, at lower values of $f_{H_2O}$, the ratio $f_{CH_4}/f_{CO_2}$ is smaller and $f_{O_2}$ is larger than at higher values of $f_{H_2O}$. The maximum value of $f_{O_2}$ for sample 48f is on the order of $10^{-23}$ at 550°C, which is close to the value for the quartz–magnetite–fayalite buffer. The graphite-free rocks from Mayhew Lake (samples 35) were probably metamorphosed under more oxidizing conditions, and the coexisting fluid consisted almost entirely of $H_2O$ and $CO_2$. Samples 39a,b,c from Loon Lake appear to have equilibrated with a relatively pure-$H_2O$ fluid. These samples were collected near a fault zone that was active during the emplacement of the Duluth Complex, and the compositions of the fluids percolating through the fault zone appear to have been very different from the compositions of 'local' fluids.

The relatively large amount of $CO_2$ in the fluid phase and the prevailing $f_{O_2}$ near the quartz–magne-

tite–fayalite buffer are consistent with the suggestions of Floran and Papike (1978) and Simmons et al. (1974) for the composition of the fluid phase during metamorphism of the underlying iron-formation. The fluid phase may have communicated with a large volume of rock during contact metamorphism; indeed, the assumption that $P_{fluid} = P_{solid}$ may not be valid for low-pressure contact metamorphism. The effect of permeability ($P_{fluid} < P_{solid}$) on the calculation of the fluid composition is to increase $X_{H_2O}$, $f_{CH_4}/f_{CO_2}$, and $f_{H_2}$, and to decrease $f_{O_2}$. For example, in sample 48f, if the fluid pressure was 1000 bars (instead of 1500 bars) $X_{H_2O}$ = 0.69, $f_{CH_4}$ = 125 bars, $f_{CO_2}$ = 287 bars, $f_{O_2}$ = 4 × $10^{-24}$ bars, $f_{H_2}$ = 9.5 bars, and $f_{CO}$ = 1.7 bars.

Table 5. Fluid composition for sample 48f

| $f_{H_2O}$ | $f_{CO_2}$ | $f_{CH_4}$ | $f_{CO}$ | $f_{H_2}$ | $f_{O_2}$ | $X_{H_2O}$ | $X_{CO_2}$ |
|---|---|---|---|---|---|---|---|
| 379[1] | 786 | 46 | 2.8 | 5.7 | 1.2 × $10^{-23}$ | 0.54 | 0.44 |
| 483[1] | 292 | 200 | 1.7 | 12 | 4.3 × $10^{-24}$ | 0.76 | 0.16 |
| 200[2] | 1250 | 8 | 3.5 | 4.2 | 1.8 × $10^{-23}$ | 0.31 | 0.69 |

[1] Range in the maximum values of $f_{H_2O}$ derived from maximum possible temperature of 544°C
[2] Values calculated for a temperature of 500°C to show effect of lower temperature on fluid composition
p = 1500 bars

## Summary

The contact metamorphic effects of the Duluth Complex on the argillaceous Rove Formation are confined to the region within a few hundred meters of the contact. In this region the low-grade assemblage chlorite + muscovite + quartz reacted to form the medium-grade assemblage cordierite + biotite + microcline. Locally adjacent to the Duluth Complex the high-grade assemblages corundum + microcline and hypersthene + cordierite formed.

The compositions of the coexisting minerals in the medium-grade assemblage biotite + cordierite + microcline provide estimates of the maximum values of temperature and partial pressure of $H_2O$ at 1500 bars. These values indicate that medium-grade assemblages formed in the range 500° to 600°C and that for most samples $P_{H_2O} \simeq \frac{1}{2}P_{solid}$. The compositions of coexisting cordierite and biotite are sensitive to variations in $f_{H_2O}$. On the basis of texture, distance from high-grade area, and partitioning of Na and K between muscovite and microcline, sample 35f formed at a lower temperature than sample 39a, but sample 35f contains a more dehydrated, higher-grade assemblage than 39a.

The contact metamorphic effects of the Duluth Complex on the Rove Formation contrast sharply with the effects on the Gunflint Iron Formation. The iron-formation preserves prograde reactions as far as 10 km from the contact. The differences between the iron-formation and the Rove Formation are, in part, the result of the large number of iron silicates that may occur in rocks poor in aluminum and potassium. The pelitic Rove Formation lacks a variety of assemblages and records few reactions because in low-pressure, contact metamorphic aureoles the assemblage biotite + cordierite + microcline is stable over large ranges in Mg/(Mg + Fe), in $T$, and in $f_{H_2O}$.

The iron-formation appears to have attained temperatures as high as 800°C. Medium-grade Rove Formation records maximum temperatures of 600°C, but no reliable estimates of metamorphic temperature of the high-grade region can be made. There is no evidence of partial melting of the high-grade Rove Formation, but the minimum melting temperature of the assemblage quartz + biotite + plagioclase + hypersthene under the condition $P_{H_2O} < P_{solid}$ is probably greater than 800°C (Luth, 1967). Because all other factors regarding the depth of emplacement and temperature of the magma at emplacement are equal, the differences in temperatures recorded by the iron-formation and Rove Formation at equivalent distances from the contact must be due to differences in the thermal properties and permeabilities of the two rock types.

## References

Albee, A. L. (1972) Metamorphism of pelitic schists: reaction relations of chloritoid and staurolite. Geological Society of America Bulletin, 83, 3249–3268.

Albee, A. L. and Ray, L. (1970) Correction factors for electron probe microanalysis of silicates, oxides, carbonates, phosphates, and sulfates. Analytical Chemistry, 42, 1408–1414.

Bence, A. E. and Albee, A. L. (1968) Empirical correction factors for electron microanalysis of silicates and oxides. Journal of Geology, 76, 382–403.

Bonnichsen, B. (1968) General geology and petrology of the metamorphosed Biwabik Iron Formation, Dunka River area, Minnesota. Ph.D. Thesis, University of Minnesota, Minneapolis, Minnesota.

Bonnichsen, B. (1969) Metamorphic pyroxenes and amphiboles in the Biwabik Iron Formation, Dunka River area, Minnesota. Mineralogical Society of America Special Paper, 2, 217–241.

Bosma, W. (1974) The posts in the spotted slates of Stiege (Vosges) and Vogtland (Saxony). Geologie en Mijnbouw, 43, 476–489.

Burnham, C. W., Holloway, J. R., and Davis, N. F. (1969) Thermodynamic properties of water to 1,000°C and 10,000 bars. Geological Society of America Special Paper 132.

Chatterjee, N. D. and Froese, E. (1975) A thermodynamic study of the pseudobinary join muscovite–paragonite in the system $KAlSi_3O_8$–$NaAlSi_3O_8$–$Al_2O_3$–$SiO_2$–$H_2O$. American Mineralogist, 60, 985–993.

Compton, R. R. (1960) Contact metamorphism in the Santa Rosa Range, Nevada. Geological Society of America Bulletin, 71, 1383–1416.

Eugster, H. P. (1977) Compositions and thermodynamics of metamorphic solutions. In D. G. Fraser, Ed., Thermodynamics in Geology, p. 183–202. D. Reidel Publishing Company, Dordrecht, The Netherlands.

Eugster, H. P., Albee, A. L., Bence, A. E., Thompson, Jr., J. B., and Waldbaum, D. R. (1972) The two-phase region and excess mixing properties of paragonite–muscovite crystalline solutions. Journal of Petrology, 13, 147–179.

Floran, R. J. and Papike, J. J. (1975) Petrology of the Gunflint Iron Formation Ontario–Minnesota: the low grade rocks. Geological Society of America Bulletin, 86, 1169–1190.

Floran, R. J. and Papike, J. J. (1978) Mineralogy and petrology of the Gunflint Iron Formation, Minnesota–Ontario: correlation of compositional and assemblage variations at low to moderate grade. Journal of Petrology, 19, 215–288.

French, B. M. (1968) Progressive contact metamorphism of the Biwabik Iron-Formation, Mesabi Range, Minnesota. Minnesota Geological Survey Bulletin 45.

Guidotti, C. V., Cheney, J. T., and Conatore, P. D. (1975a) Coexisting cordierite + biotite + chlorite from the Rumford Quadrangle, Maine. Geology, 3, 147–148.

Guidotti, C. V., Cheney, J. T., and Conatore, P. D. (1975b) Inter-relationship between Mg/Fe ratio and octahedral Al content in biotite. American Mineralogist, 60, 849–853.

Labotka, T. C. (1978) Geology of the Telescope Peak Quadrangle, California, and Regional Metamorphism in the Death Valley Area, California. Ph.D. Thesis, California Institute of Technology, Pasadena, California.

Luth, W. C. (1967) Studies in the system $KAlSiO_4-Mg_2SiO_4-SiO_4-H_2O$: I, inferred phase relations and petrologic applications. Journal of Petrology, 8, 372–416.

Miyashiro, A. (1958) Regional metamorphism in the Gosaisyo-Takanuki district in the central Abukuma Plateau. Tokyo University Faculty Science Journal, 11, 219–272.

Morey, G. B. (1969) The geology of the Middle Precambrian Rove Formation in northeastern Minnesota. Minnesota Geological Survey Special Publication 7.

Morey, G. B., Papike, J. J., Smith, R. W., and Weiblen, P. W. (1972) Observations on the contact metamorphism of the Biwabik Iron-Formation, East Mesabi district, Minnesota. Geological Society of America Memoir, 135, 225–264.

Okrusch, M. (1969) Die Gneishornfelse um Steinach in der Oberpfalz. Eine phasenpetrologische Analyse. Contributions to Mineralogy and Petrology, 22, 32–72.

Powell, M. and Powell, R. (1977) Plagioclase–alkali feldspar geothermometry revisited. Mineralogical Magazine, 41, 253–256.

Read, H. H. (1952) Metamorphism and migmatisation in the Ythan Valley, Aberdeenshire. Transactions of the Edinburgh Geological Society, 15, 265–279.

Schreyer, W. and Seifert, F. (1967) Metastability of an osumilite end-member in the system $K_2O-MgO-Al_2O_3-SiO_2-H_2O$ and its possible bearing on the rarity of natural osumilites. Contributions to Mineralogy and Petrology, 14, 343–358.

Schreyer, W. and Seifert, F. (1969) Compatibility relations of the aluminum silicates in the system $MgO-Al_2O_3-SiO_2-H_2O$ and $K_2O-MgO-Al_2O_3-SiO_2-H_2O$ at high pressures. American Journal of Science, 267, 371–388.

Scott, S. D. (1973) Experimental calibration of the sphalerite geobarometer. Economic Geology, 68, 466–474.

Scott, S. D. (1975) Sulphide geothermometers and geobarometers. (abstr.) International Conference on Geothermometry and Geobarometry, Pennsylvania State University, University Park, Pennsylvania.

Simmons, E. C., Lindsley, D. H., and Papike, J. J. (1974) Phase relations and crystallization sequence in a contact-metamorphosed rock from the Gunflint Iron Formation, Minnesota. Journal of Petrology, 15, 539–565.

Stormer, J. C. (1975) A practical two-feldspar thermometer. American Mineralogist, 60, 667–674.

Thompson, A. B. (1974) Calculation of muscovite–paragonite–alkali feldspar phase relations. Contributions to Mineralogy and Petrology, 44, 173–194.

Thompson, J. B. (1957) The graphical analysis of mineral assemblages in pelitic schists. American Mineralogist, 42, 842–858.

Tilley, C. E. (1924) Contact metamorphism in the Comrie area of the Perthshire Highlands. Quarterly Journal of the Geological Society of London, 81, 100–112.

Waldbaum, D. R. and Thompson, Jr., J. B. (1969) Mixing properties of sanidine crystalline solutions: IV. Phase diagrams from equation of state. American Mineralogist, 54, 1274–1298.

Weiblen, P. W., Mathez, E. A., and Morey, G. B. (1972) Logan intrusions. In P. D. Sims and G. B. Morey, Eds., Geology of Minnesota: A Centennial Volume, p. 394–406. Minnesota Geological Survey, St. Paul, Minnesota.